Steel and Composite Structures, Vol. 4, No. 6 (2004) 489-507
DOI: http://dx.doi.org/10.12989/scs.2004.4.6.489

Non-linear analysis of composite steel-concrete beams with incomplete interaction

Bojan Čas†, Sebastjan Bratina†, Miran Saje‡ and Igor Planinc‡†

University of Ljubljana, Faculty of Civil and Geodetic Engineering, Jamova 2, SI-1115 Ljubljana, Slovenia

Abstract. The flexibility of the connection between steel and concrete largely influences the global behaviour of the composite beam. Therefore the way the connection is modelled is the key issue in its structural analysis. Here we present a new strain-based finite element formulation in which we consider non-linear material and contact models. The computational efficiency and accuracy of the formulation is proved with the comparison of our numerical results with the experimental results of Abdel Aziz (1986) obtained in a full-scale laboratory test. The shear connectors are assumed to follow a non-linear load–slip relationship proposed by Ollgaard *et al.* (1971). We introduce the notion of the generalized slip, which offers a better physical interpretation of the behaviour of the contact and gives an additional material slip parameter. An excellent agreement of experimental and numerical results is obtained, using only a few finite elements. This demonstrates that the present numerical approach is appropriate for the evaluation of behaviour of planar composite beams and perfect for practical calculations.

Key words: steel-concrete composite beam; shear connection; interlayer slip; non-linear analysis; finite element method.

1 Introduction

Steel-concrete beams are widely used for floor constructions in buildings and bridges due to their economy of construction and good bearing capacity. The theoretical analysis of the mechanical behaviour of these structures is rather complex. A number of theoretical and numerical models for the steel-concrete beams have been proposed in literature. Razaqpur and Nofal (1989) and Wegmuller and Amer (1997) employed the 2D and 3D analyses to model the behaviour of steel-concrete structures. Such analyses are computationally very demanding. The 1D analyses model concrete and steel layers as the beams connected together in such a way that their transverse displacements are fully compatible, see, e.g., the pioneering works by Newmark *et al.* (1951) and Adekola (1968) or the recent work by Ayoub (2001). Since 1988 when Robinson and Naraine demonstrated that the delamination of the concrete and steel layers had a negligible effect on behaviour of the composite structure, most researchers have assumed that the layers slip over each other without any transverse separation.

After many experiments (e.g., Aribert and Abdel Aziz 1985, Abdel Aziz 1986), it is now recognized that the behaviour of the composite steel-concrete structures is inherently non-linear. The corresponding

†Assistant
‡Professor, Corresponding Author, E-mail: msaje@fgg.uni.lj.si
‡†Assistant Professor

mathematical models must also be non-linear, which requires numerical solution methods to be used, although some rare analytical solutions of simplified linear models are also of great value (e.g., Girhammar *et al.* 1993, Ranzi *et al.* 2003). One among more important numerical solution methods found in literature is the finite element method. Various finite element formulations have been proposed for the solution of steel-concrete composite structures, which differ in the way the variational principles and the basic variables are chosen. Dall'Asta and Zona (2002), Daniel and Crisinel (1993) and Gattesco (1999) proposed the displacement-based formulations; Salari *et al.* (1998) proposed the finite element formulation, where the forces are basic variables, while Ayoub and Filippou (2000) and Ayoub (2001) employed both the displacements and the forces.

In the present paper we introduce a new finite element model of a layered composite beam, which we prove to be both reliable and computationally efficient. As pointed out by Fabroccino *et al.* (1999), any solution must necessarily consider the slip between the concrete slab and the steel girder, and the non-linear constitutive relationship for shear connectors. Therefore, we consider the slip between the layers and assume that the behaviour of materials and the shear connectors is non-linear. We assume that the transverse separation between the layers is not possible and that the interaction between the layers is fully driven by the load–slip characteristic of the connector. We further assume that the beam is planar and that each layer suffers small deformations so that the geometrically linear beam model is sufficient. The mathematical model of the composite beam is described by a set of algebraic-differential equations and boundary conditions, which we solve numerically by the finite element method.

Our finite element formulation employs a modified principle of virtual work, in which the basic unknown functions are strains, not displacements or forces. We use the concept of the consistent equilibrium of constitutive and equilibrium-based stress-resultants (Vratanar and Saje 1999), and employ the Galerkin type of the finite element formulation (Planinc 1998). Displacements and rotations are not interpolated in our formulation.

In a composite structure, the upper layer is constrained to follow the deformation of the lower layer. When deforming, the layers slip over each other, but the transverse separation between them does not occur. The slip is traditionally understood as the actual slip between the two materials, concrete and steel, see, e.g., Gattesco and Giuriani (1996) or Ollgaard *et al.* (1971). By contrast, the slip in the present paper is defined in a generalized way as an 'average slip' over a thin sublayer of the softer material layer rather than at the actual contact. Such a 'generalized slip' takes place over a concrete sublayer neighbouring the steel girder. The thickness of the sublayer depends on the stiffness of the connector and on the strength of concrete, and must be found experimentally. Once obtained, the generalized slip is used in the force-slip relationship of Ollgaard *et al.* (1971). The introduction of the generalized slip offers a better physical interpretation of the slip and adds a new material parameter to the mathematical model.

We verify the present formulation by comparing our numerical results to the results of a fullscale experiment on a composite beam made from a reinforced concrete slab and a steel girder connected together by the Nelson studs (Abdel Aziz 1986).

2. Basic equations of composite beam

We assume that the planar beam is made from two layers, connected together in such a way that slip of one layer over the other is possible, while the transverse separation is not. Each layer modelled by

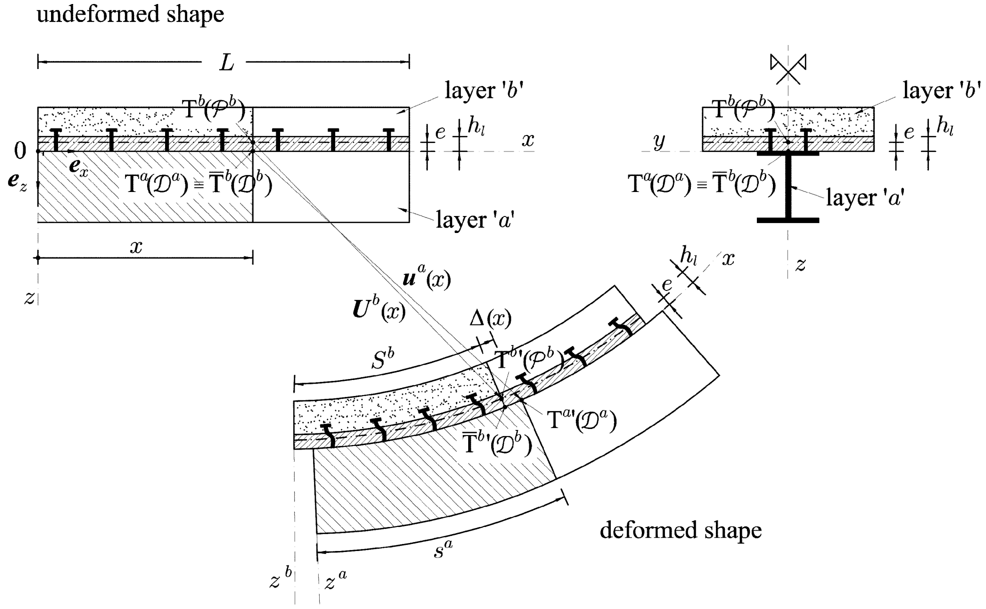

Fig. 1 Undeformed and deformed shapes of the two-layer composite beam

the linearized beam theory, in which plane cross-sections remain planar during deformation, and shear strains are neglected.

We consider an intially straight composite beam of undeformed length L: The beam lies in the (x, z)-plane of the Cartesian coordinate system (x, y, z) with the unit base vectors e_x, e_z and $e_y = e_z \times e_x$. The common reference axis of the layers is taken to lie in their contact plane. The composite beam is subjected to the action of the distributed load $p = p_x e_x + p_z e_z$ and the distributed moment load $m = m_y e_y$ along the reference axis of layer b, and to concentrated generalized loads S_i^a and S_i^b $(i = 1, 2, \ldots, 6)$ at its ends. The loading is assumed to be deformation-independent.

Let two particles, one from layer a and the other from layer b, be in contact in the underformed state and occupy the same point (x, y, z) in space. After the deformation takes place, the positions of these particles become different and are described by the position vectors (Fig. 1)

$$\boldsymbol{R}^a(x, z) = (x + u^a(x) + z\varphi^a(x))e_x + (z + w^a(x))e_z \tag{1}$$

$$\boldsymbol{R}^b(x, z) = (x + u^b(x) + z\varphi^b(x))e_x + (z + w^b(x))e_z \tag{2}$$

Functions u^a and w^a denote the components of the displacement vector of the reference axis of layer a with respect to base vectors e_x and e_z. Similarly, components u^b and w^b belong to the displacement vector of the reference axis of layer b. Functions φ^a and φ^b are the rotations of reference axes of layers a and b, respectively. For the later convenience, we also introduce the notations for the components of the displacement vectors of a generic particle (x, z) of layers a and b:

$$U^a(x, z) = u^a(x) + z\varphi^a(x), \qquad U^b(x, z) = u^b(x) + z\varphi^b(x) \tag{3}$$

$$W^a(x, z) = w^a(x), \qquad W^b(x, z) = w^b(x) \tag{4}$$

The basic equations of the composite beam consist of *kinematic*, *equilibrium* and *constitutive* equations with boundary equations for each of the two layers, and the *constraining equations* that assemble layers into a composite structure. In what follows, we list these equations without going into details of their derivations.

2.1. Kinematic equations

We assume that the plane cross-section of each layer remains planar and perpendicular to its deformed reference axis. We further assume that strains and displacements are small. Then the kinematic equations of the layers read:

$$u^{a'} - \varepsilon^a = 0, \qquad u^{b'} - \varepsilon^b = 0 \tag{5}$$

$$w^{a'} + \varphi^a = 0, \qquad w^{b'} + \varphi^b = 0 \tag{6}$$

$$\varphi^{a'} - \kappa^a = 0, \qquad \varphi^{b'} - \kappa^b = 0 \tag{7}$$

ε^a, ε^b are the extensional (membrane) strains, and κ^a, κ^b are the bending strains (pseudocurvatures) of the reference axes of layers *a* and *b*, respectively. In Eqs. (5)-(7) and throughout the text, the prime (') denotes the derivative with respect to *x*.

2.2. Equilibrium equations

The equilibrium equations read:

$$\mathcal{N}^{a'} + q_x^a = 0, \qquad \mathcal{N}^{b'} + q_x^b + p_x = 0 \tag{8}$$

$$\mathcal{Q}^{a'} + q_z^a = 0, \qquad \mathcal{Q}^{b'} + q_z^b + p_z = 0 \tag{9}$$

$$\mathcal{M}^{a'} - \mathcal{Q}^a = 0, \qquad \mathcal{M}^{b'} - \mathcal{Q}^b + m_y = 0 \tag{10}$$

In these equations, $\mathcal{N}^a$, $\mathcal{N}^b$, $\mathcal{Q}^a$, $\mathcal{Q}^b$, $\mathcal{M}^a$ and $\mathcal{M}^b$ denote the equilibrium axial forces, shear forces and bending moments in layers *a* and *b*; q_x^a, q_x^b, q_z^a and q_z^b are the *x*- and *z*-components of the contact traction in the plane of contact between the layers.

2.3. Constitutive equations

In addition to the equilibrium axial forces and moments, we also introduce the constitutive axial forces and moments, $\mathcal{N}_c^a$, $\mathcal{N}_c^b$ and $\mathcal{M}_c^a$, $\mathcal{M}_c^b$ of layers *a* and *b*. These are the cross-sectional stress-resultants determined from strains with the help of the constitutive equations. We know that these two sets of internal forces and moments must coincide:

$$\mathcal{N}^a = \mathcal{N}_c^a, \qquad \mathcal{N}^b = \mathcal{N}_c^b \tag{11}$$

$$\mathcal{M}^a = \mathcal{M}_c^a, \qquad \mathcal{M}^b = \mathcal{M}_c^b \tag{12}$$

2.4. Boundary equations

As the kinematic and the equilibrium equations are differential, we need the boundary conditions for each layer. These are either the natural (force) or the essential (displacement) boundary conditions. For layer a they read:

$$x = 0: \quad S_1^a + \mathcal{N}^a(0) = 0 \quad \text{or} \quad u^a(0) = u_1^a \tag{13}$$

$$S_2^a + \mathcal{Q}^a(0) = 0 \quad \text{or} \quad w^a(0) = u_2^a \tag{14}$$

$$S_3^a + \mathcal{M}^a(0) = 0 \quad \text{or} \quad \varphi^a(0) = u_3^a \tag{15}$$

$$x = L: \quad S_4^a - \mathcal{N}^a(L) = 0 \quad \text{or} \quad u^a(L) = u_4^a \tag{16}$$

$$S_5^a - \mathcal{Q}^a(L) = 0 \quad \text{or} \quad w^a(L) = u_5^a \tag{17}$$

$$S_6^a - \mathcal{M}^a(L) = 0 \quad \text{or} \quad \varphi^a(L) = u_6^a \tag{18}$$

In Eqs. (13)–(18) u_i^a (i = 1, 2,..., 6) mark the given values of the generalized boundary displacements and S_i^a (i = 1, 2,..., 6) the given values of generalized forces at the edges $x = 0$ and $x = L$ of layer a. An analogous set of the boundary conditions holds for layer b.

2.5. Constraining equations

Once the layers are connected together, the upper layer is constrained to follow the deformation of the lower layer in such a way that the layers can slip over each other, but the transverse separation between them is not possible. The 'slip' here is understood in a generalized way. When the layers are relatively stiff compared to the connector or if they are not connected at all (as in dry friction), then the slip occurs along the contact. When one of the layers is much softer than the other, the major part of the 'slip' occurs in the layer of the softer material. This case takes place in composite beams made from steel and concrete connected by steel shear studs; there, due to the strong steel shear studs, the slip at the contact between concrete and steel is practically negligible, and realizes only over a concrete sublayer neighbouring the steel beam. The thickness of the sublayer depends on the stiffness of studs and the strength of concrete, and is roughly equal to the length of the stud. The sublayer will be called the 'slip sublayer', while the average slip in the sublayer will be called the 'generalized slip'. The generalized slip is defined as the tangential displacement between the deformed positions of an 'average' particle $\mathcal{P}^b$ inside the slip sublayer and steel particle $\mathcal{D}^a$ on the contact surface, which - in the undeformed state- lies in the same cross-section as particle $\mathcal{P}^b$ (see Fig. 1 for the precise definition of the particles). It is denoted by Δ and evaluated as $\Delta = s^a - S^b$, where s^a is the deformed arc-length of the reference axis of layer a, and S^b is the deformed arc-length of the curve through particle $\mathcal{P}^b$, parallel to the axis of layer b, and being 'e' away from the reference axis (Fig. 1). Thus:

$$\Delta(x) = s^a(x) - S^b(x) = s^a(0) - S^b(0) + \int_0^x (\varepsilon^a - D^b)d\xi = \Delta(0) + \int_0^x (\varepsilon^a - D^b)d\xi \tag{19}$$

$\mathcal{D}^b$ is extensional strain at $\mathcal{P}^b$, which is related to the x-displacement component of the particle by the kinematic equation

$$\mathcal{D}^b = U^{b\prime} \tag{20}$$

Inserting ε^a and $\mathcal{D}^b$ from Eqs. (5a) and (20), integrating and considering relations $s^a(0)=u^a(0)$, $S^b(0) = U^b(0)$ and $\Delta(0)=u^a(0)-U^b(0)$ in Eq. (19), gives:

$$\Delta(x) = \Delta(0) + \int_0^x (\varepsilon^a - D^b) d\xi = u^a(x) - U^b(x) \tag{21}$$

The condition that there is no transverse separation between the layers requires that the two particles $\mathcal{D}^a$ and $\mathcal{D}^b$ which are in contact in the deformed shape, have equal position vectors. Thus, $\boldsymbol{r}^a(x)=\boldsymbol{r}^b(x^*)$, or in the componential form

$$x + u^a(x) = x^* + u^b(x^*) \tag{22}$$

$$w^a(x) = w^b(x^*) \tag{23}$$

Here $x^* \in \mathcal{I}^{b*}$ denotes the undeformed coordinate of that particle $\mathcal{D}^b$ of layer b which, in the deformed state, coincides with the particle $\mathcal{D}^a$ of layer a having coordinate $x \in \mathcal{I}^a$. $\mathcal{I}^a$ and $\mathcal{I}^{b*}$ denote the effective regions of contact between layers a and b.

The layers act onto each other with the tractions, which will be denoted by $\boldsymbol{q}^a$ and $\boldsymbol{q}^b$. Since we have assumed that the rotations are small ($\sin\varphi \approx \varphi$), the traction components with respect to the tangent and the normal of the contact surface, q_t^a, q_n^a, q_t^b and q_n^b, are related to the components with respect to the (x, y, z)-system with the following equations:

$$q_x^a(x) \cong q_t^a(x) \tag{24}$$

$$q_z^a(x) \cong q_n^a(x) \tag{25}$$

$$q_x^b(x^*) \cong q_t^b(x^*) \tag{26}$$

$$q_z^b(x^*) \cong q_n^b(x^*) \tag{27}$$

The normal traction component satisfies the equation

$$q_n^a(x) + q_n^b(x^*) = 0 \tag{28}$$

In view of the small strain and small slip assumptions, the further simplifications

$$q_t^a(x) + q_t^b(x^*) = 0 \tag{29}$$

$$q_t^b(x^*) \cong q_t^b(x) \tag{30}$$

$$q_n^b(x^*) \cong q_n^b(x) \tag{31}$$

are acceptable. Inserting Eqs. (28)-(29) and (30)-(31) into (24)-(27) yields

$$q_x^b(x) = -q_x^a(x) = q_t^b(x) = -q_t^a(x) = q_t \tag{32}$$

$$q_z^b(x) = -q_z^a(x) = q_n^b(x) = -q_n^a(x) = q_n \tag{33}$$

2.6 Constitutive equations of the connection

In the light of the discussion in the subsection *Constraining equations*, we assume that the tangential contact traction q_t depends on the generalized (average) slip, whose action takes place in the fibre e away from the actual contact surface (see Fig. 1). We then have

$$q_t = \mathcal{F}(\Delta) \tag{34}$$

Here $\mathcal{F}(\Delta)$ is a non-linear functional of $\Delta(x)$ to be determined by an experiment. The tangential contact traction depends on an experimentally evaluated position of the generalized slip, therefore the position of the generalized slip, e, and the resultant tangential contact traction have to be measured in this experiment.

Constraining Eqs. (21)–(23), (28), (29) and (34) represent additional six equations for the six unknown functions: Δ, q_t^a, q_t^b, q_n^a, q_n^b and x^*. In what follows q_t will be denoted by q.

2.7. Further simplifications and the final form of the governing equations of the composite beam

When strains, displacements, rotations and slips are small quantities, we can assume that

$$dx \cong dx^* \tag{35}$$

$$\mathcal{I}^a = \mathcal{I}^{b^*} = [0, L] \tag{36}$$

which yields the fact that the bending strains of the layers are equal: $\kappa^a(x) = \kappa^b(x^*)$. This implies the equality $(\bullet)^b(x^*) \cong (\bullet)^b(x)$ for any mechanical quantity of layer b. Consequently, the kinematic, equilibrium and constitutive equations become very simple. First, as a consequence of assuming $w^a(x) = w^b(x^*) = w^b(x)$ in Eq. (23), we derive $\varphi^a(x) = \varphi^b(x^*) = \varphi^b(x)$ and $\kappa^a(x) = \kappa^b(x^*) = \kappa^b(x)$. Hence Eqs. (6) of both layers become identical and reduce to one equation

$$w' + \varphi = 0 \tag{37}$$

where $w(x) = w^a(x) = w^b(x)$ and $\varphi(x) = \varphi^a(x) = \varphi^b(x)$: Similarly, Eq. (7) can be replaced by

$$\varphi' - \kappa = 0 \tag{38}$$

where $\kappa(x) = \kappa^a(x) = \kappa^b(x)$ is the bending strain of the composite beam. Next, by combining Eqs. (25), (27) and (28), we obtain

$$q_z^a(x) + q_z^b(x) = 0 \tag{39}$$

We find it convenient to introduce the equilibrium shear force, $\mathcal{Q}$, and the equilibrium bending moment, $\mathcal{M}$, of the composite cross-section. $\mathcal{Q}$ is defined as the sum of the equilibrium shear forces of layers a and b: $\mathcal{Q} = \mathcal{Q}^a + \mathcal{Q}^b$. The differentiation of $\mathcal{Q}$ with respect to x and the consideration of Eq. (9) yields

$$\mathcal{Q}' + p_z = 0 \tag{40}$$

Similarly, from the moment quilibrium Eqs. (10) we obtain

$$\mathcal{M}' - \mathcal{Q} + m_y = 0 \tag{41}$$

Here $\mathcal{M}=\mathcal{M}^a+\mathcal{M}^b$ is the bending moment of the composite cross-section of the beam.

The final governing differential and algebraic equations of the composite beam are displayed in Box 1. For a given external loading, Eqs. (43)-(56) constitute a system of 14 algebraic-differential equations for 14 unknown functions $u^a(x)$, $u^b(x)$, $w(x)$, $\varphi(x)$, $\varepsilon^a(x)$, $\varepsilon^b(x)$, $\kappa(x)$, $\mathcal{N}^a(x)$, $\mathcal{N}^b(x)$, $\mathcal{Q}(x)$, $\mathcal{M}(x)$, $\Delta(x)$, $q(x)$ and $x^*(x)$ along with the natural and essential boundary conditions (57)-(64). Eq. (55) appears to be fully separated and can thus be solved after the analysis has been completed.

As some of the governing equations are non-linear (see Eqs. (51)-(53) and (56)), we solve the equations numerically with the finite element method, as described in the next section.

3 Finite element method

3.1. Modified principle of virtual work

The starting point of our numerical formulation is the principle of virtual work, which says that the difference of virtual works of internal and external forces is zero

$$\begin{aligned}\delta W = {} & \int_0^L (\mathcal{N}_c^a \delta\varepsilon^a + \mathcal{N}_c^b \delta\varepsilon^b + \mathcal{M}_c \delta\kappa)dx - \\ & \int_0^L (q\,\delta u^a - (p_x - q)\,\delta u^b - p_z \delta w - m_y \delta\varphi)dx - \text{ boundary terms } = 0\end{aligned} \tag{42}$$

Box 1: Governing equations of the composite beam

Kinematic equations:	$u^{a'} - \varepsilon^a = 0$	(43)
	$u^{b'} - \varepsilon^b = 0$	(44)
	$w' + \varphi = 0$	(45)
	$\varphi' - \kappa = 0$	(46)
Equilibrium equations:	$\mathcal{N}^{a'} - q = 0$	(47)
	$\mathcal{N}^{b'} + q + p_x = 0$	(48)
	$\mathcal{Q}' + p_z = 0$	(49)
	$\mathcal{M}' - \mathcal{Q} + m_y = 0$	(50)
Constitutive equations:	$\mathcal{N}^a = \mathcal{N}_c^a$	(51)

$$\mathcal{N}^b = \mathcal{N}_c^b \tag{52}$$

$$\mathcal{M} = \mathcal{M}_c = \mathcal{M}_c^a + \mathcal{M}_c^b \tag{53}$$

Constraining equations:

$$\Delta = u^a - u^b + e\varphi \tag{54}$$

$$x + u^a = x^* + u^b \tag{55}$$

$$q = \mathcal{F}(\Delta) \tag{56}$$

Natural and essential boundary conditions:

$x = 0$:

$$S_1^a + \mathcal{N}^a(0) = 0 \quad \text{or} \quad u^a(0) = u_1^a \tag{57}$$

$$S_1^b + \mathcal{N}^b(0) = 0 \quad \text{or} \quad u^b(0) = u_1^b \tag{58}$$

$$S_2 + \mathcal{Q}(0) = 0 \quad \text{or} \quad w(0) = u_2 \tag{59}$$

$$S_3 + \mathcal{M}(0) = 0 \quad \text{or} \quad \varphi(0) = u_3 \tag{60}$$

$x = L$:

$$S_4^a - \mathcal{N}^a(L) = 0 \quad \text{or} \quad u^a(L) = u_4^a \tag{61}$$

$$S_4^b - \mathcal{N}^b(L) = 0 \quad \text{or} \quad u^b(L) = u_4^b \tag{62}$$

$$S_5 - \mathcal{Q}(L) = 0 \quad \text{or} \quad w(L) = u_5 \tag{63}$$

$$S_6 - \mathcal{M}(L) = 0 \quad \text{or} \quad \varphi(L) = u_6 \tag{64}$$

The principle given in Eq. (42) has been derived on the basis of the assumption that the kinematic and deformation variables are constrained by the kinematic and constitutive Eqs. (43)-(46) and (11)-(12). These constraints are released if we introduce the Hu–Washizu functional with Eqs. (43)-(46) and (11)-(12) as the constraining equations of the functional. Assuming further that Eqs. (43)-(50) are identically satisfied, and extending the functional with the boundary kinematic constraints, we derive the principle, which we call the modified principle of virtual work (Planinc 1998):

$$\delta W^* = \int_0^L ((\mathcal{N}_c^a - \mathcal{N}^a)\delta\varepsilon^a + (\mathcal{N}_c^b - \mathcal{N}^b)\delta\varepsilon^b + (\mathcal{M}_c - \mathcal{M})\delta k)dx +$$

$$(u^a(L) - u^a(0) - \int_0^L \varepsilon^a dx)\delta\mathcal{N}^a(0) + (u^b(L) - u^b(0) - \int_0^L \varepsilon^b dx)\delta\mathcal{N}^b(0) +$$

$$(w(L) - w(0) + \int_0^L \varphi dx)\delta\mathcal{Q}(0) - (\varphi(L) - \varphi(0) - \int_0^L k dx)\delta M(0) -$$

$$\text{boundary terms} = 0: \tag{65}$$

The functional in Eq. (65) depends on the values of the forces and moment at x=0, i.e., $\mathcal{N}^a(0)$, $\mathcal{N}^b(0)$, $\mathcal{Q}(0)$ and $\mathcal{M}(0)$, the boundary displacements and rotations, $u^a(0)$, $u^b(0)$, $w(0)$, $\varphi(0)$, $u^a(L)$, $u^b(L)$, $w(L)$ and $\varphi(L)$, the extensional strains of the reference axes of layers a and b, $\varepsilon^a(x)$ and $\varepsilon^b(x)$, and the bending strain of the composite beam, $\kappa(x)$. In the finite element implementation of the principle, we need to interpolate three deformation functions, $\varepsilon^a(x)$, $\varepsilon^b(x)$ and $\kappa(x)$.

3.2. Finite element method

The reference axis of the composite structure is divided into finite elements. Within each element, the extensional strains ε^a and ε^b of layers a and b, and the bending strain κ are interpolated by Lagrangian polynomials $L_i(x)$ (i=1; 2,..., N) of order N–1 with equidistant nodes:

$$\varepsilon^a(x) = L_1(x)\varepsilon_1^a + L_2(x)\varepsilon_2^a + \ldots + L_N(x)\varepsilon_N^a \tag{66}$$

$$\varepsilon^b(x) = L_1(x)\varepsilon_1^b + L_2(x)\varepsilon_2^b + \ldots + L_N(x)\varepsilon_N^b \tag{67}$$

$$\kappa(x) = L_1(x)\kappa_1 + L_2(x)\kappa_2 + \ldots + L_N(x)\kappa_N \tag{68}$$

ε_i^a, ε_i^b and κ_i (i=1, 2,..., N) are the nodal values of $\varepsilon^a(x)$, $\varepsilon^b(x)$ and $\kappa(x)$. With the interpolations (66)–(68) the kinematic Eqs. (43)–(46) can easily be analytically integrated to yield the displacements and the rotation at any point of the beam:

$$u^a(x) = u^a(0) + P_1(x)\varepsilon_1^a + P_2(x)\varepsilon_2^a + \ldots + P_N(x)\varepsilon_N^a \tag{69}$$

$$u^b(x) = u^b(0) + P_1(x)\varepsilon_1^b + P_2(x)\varepsilon_2^b + \ldots + P_N(x)\varepsilon_N^b \tag{70}$$

$$\varphi(x) = \varphi(0) + P_1(x)\kappa_1 + P_2(x)\kappa_2 + \ldots + P_N(x)\kappa_N \tag{71}$$

$$w(x) = w(0) - \varphi(0)x - I_1(x)\kappa_1 - I_2(x)\kappa_2 - \ldots - I_N(x)\kappa_N \tag{72}$$

In the above equations, $P_i(x) = \int_0^x L_i(\xi)d\xi$ and $I_i(x) = \int_0^x P_i(\xi)d\xi$ (i = 1,2,..., N).

Once the displacements are known, the slip $\Delta(x)$ is determined from Eq. (54) and inserted into Eq. (56) to obtain the traction $q(x)=\mathcal{F}(\Delta(x))$. Putting $q(x)$ into the equilibrium Eqs. (47)-(50) and integrating, yields:

$$\mathcal{N}^a(x) = \mathcal{N}^a(0) + \int_0^x \mathcal{F}(\Delta(\xi))d\xi \tag{73}$$

$$\mathcal{N}^b(x) = \mathcal{N}^b(0) - \int_0^x (\mathcal{F}(\Delta(\xi)) - p_x(\xi))d\xi \tag{74}$$

$$\mathcal{Q}(x) = \mathcal{Q}(0) - \int_0^x p_z(\xi)d\xi \tag{75}$$

$$\mathcal{M}(x) = \mathcal{M}(0) - \int_0^x (\mathcal{Q}(\xi) - m_y(\xi))d\xi \tag{76}$$

The remaining Eqs. (51)-(53) are solved approximately by the finite element method using the modified principle of virtual work (65). Insertion of Eqs. (66)-(68) and their variations into the variational principle (65) and the vanishing of the coefficients at the variations yield the Euler-Lagrange equations of the principle. These are:

$$g_i = \int_0^L (\mathcal{N}^a - \mathcal{N}_c^a)L_i d\xi = 0\,, \qquad i = 1,\ldots, N \tag{77}$$

$$g_{N+j} = \int_0^L (\mathcal{N}^b - \mathcal{N}_c^b) L_j d\xi = 0\,, \qquad j = 1,..., N \tag{78}$$

$$g_{2N+k} = \int_0^L (\mathcal{M} - \mathcal{M}_c) L_k d\xi = 0\,, \qquad k = 1,..., N \tag{79}$$

$$g_{3N+1} = u^a(L) - u^a(0) - P_1(L)\varepsilon_1^a - P_2(L)\varepsilon_2^a - \ldots - P_N(L)\varepsilon_N^a = 0 \tag{80}$$

$$g_{3N+2} = u^b(L) - u^b(0) - P_1(L)\varepsilon_1^b - P_2(L)\varepsilon_2^b - \ldots - P_N(L)\varepsilon_N^b = 0 \tag{81}$$

$$g_{3N+3} = \varphi(L) - \varphi(0) - P_1(L)\kappa_1 + P_2(L)\kappa_2 - \ldots - P_N(L)\kappa_N = 0 \tag{82}$$

$$g_{3N+4} = w(L) - w(0) + \varphi(0)L + I_1(L)\kappa_1 + I_2(L)\kappa_2 + \ldots + I_N(L)\kappa_N = 0 \tag{83}$$

$$g_{3N+5} = S_1^a + \mathcal{N}^a(0) = 0 \tag{84}$$

$$g_{3N+6} = S_1^b + \mathcal{N}^b(0) = 0 \tag{85}$$

$$g_{3N+7} = S_2 + \mathcal{Q}(0) = 0 \tag{86}$$

$$g_{3N+8} = S_3 + \mathcal{M}(0) = 0 \tag{87}$$

$$g_{3N+9} = S_4^a - \mathcal{N}^a(0) - \int_0^L \mathcal{F}(\Delta(\xi)) d\xi = 0 \tag{88}$$

$$g_{3N+10} = S_4^b - \mathcal{N}^b(0) + \int_0^L (\mathcal{F}(\Delta(\xi)) + p_x(\xi)) d\xi = 0 \tag{89}$$

$$g_{3N+11} = S_5 - \mathcal{Q}(0) + \int_0^L p_z(\xi) d\xi = 0 \tag{90}$$

$$g_{3N+12} = S_6 - \mathcal{M}(0) + \int_0^L (\mathcal{Q}(\xi) - m_y(\xi)) d\xi = 0 \tag{91}$$

For a given load factor, λ, Eqs. (77)-(91) constitute a system of $3N$+12 non-linear algebraic equations for $3N$+12 unknowns. There are $3N$+4 internal degrees of freedom, $\varepsilon_n^a, \varepsilon_n^b$, κ_n (n=1, 2,..., N), $\mathcal{N}^a(0), \mathcal{N}^b(0)$, $\mathcal{Q}(0)$ and $\mathcal{M}(0)$, and eight external degrees of freedom, i.e., nodal displacements and rotations $u^a(0)$, $u^b(0)$, $w(0)$, $\varphi(0)$, $u^a(L)$, $u^b(L)$, $w(L)$, $\varphi(L)$ of the finite element. When $F(\Delta)$, $\mathcal{N}_c^a$, $\mathcal{N}_c^b$ and $\mathcal{M}_c$ are non-linear functionals, the integrals in Eqs. (77)-(91) are evaluated numerically by Gaussian or Lobatto's integration. For the solution of the equations, we employ the iterative Newton-Raphson method. After completing the linearization of Eqs. (77)-(91) and the construction of the tangent stiffness matrix and the residual force vector of a finite element, we assemble the global tangent stiffness matrix and the residual force vector of the structure in a classical way. Note that at least one boundary displacement in the x-direction, belonging either to layer a or b (i.e., one among $u^a(0)$, $u^a(L)$, $u^b(0)$ or $u^b(L)$), must be prescribed.

4. Numerical example

The suitability of the present theoretical approach and its numerical solution method for the analysis of real-life steel-concrete composite beams will be verified by the experimental results of a full-scale laboratory test on a simply supported beam investigated by Abdel Aziz (1986) and marked as PI4. The beam is composed from the reinforced concrete slab and the steel girder of the 'I' cross-section,

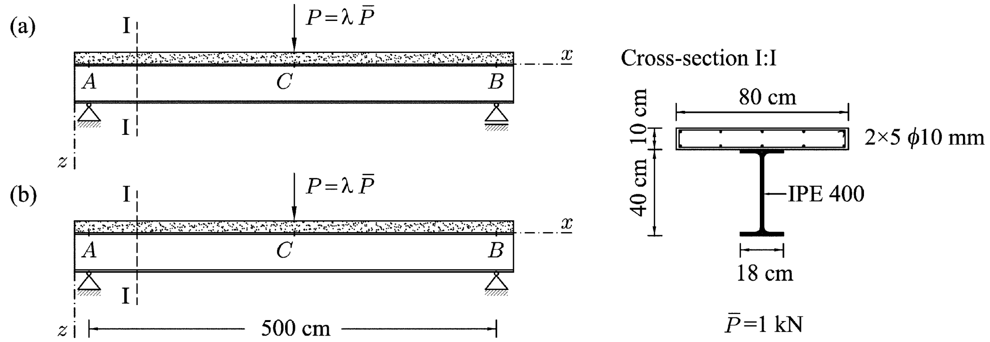

Fig. 2 Geometry, supporting and load of steel-concrete composite beam PI4

connected to each other with standard steel shear studs. This beam collapsed due to the failure of the critical cross-section, so that the lateral buckling of the steel girder, the local buckling of the steel girder flange or the delamination of the concrete slab and the steel girder can safely be neglected. Next, the experimental results show, that the deflections of the beam at about the failure load are not greater than 5% of the span. This suggests that the geometrically-linear theory as considered here suffices. We are particularly interested in assessing the capability of our model to predict the load–carrying capacity and the variation of the slip along the contact of steel and concrete. The descriptive data of the beam are given in Fig. 2.

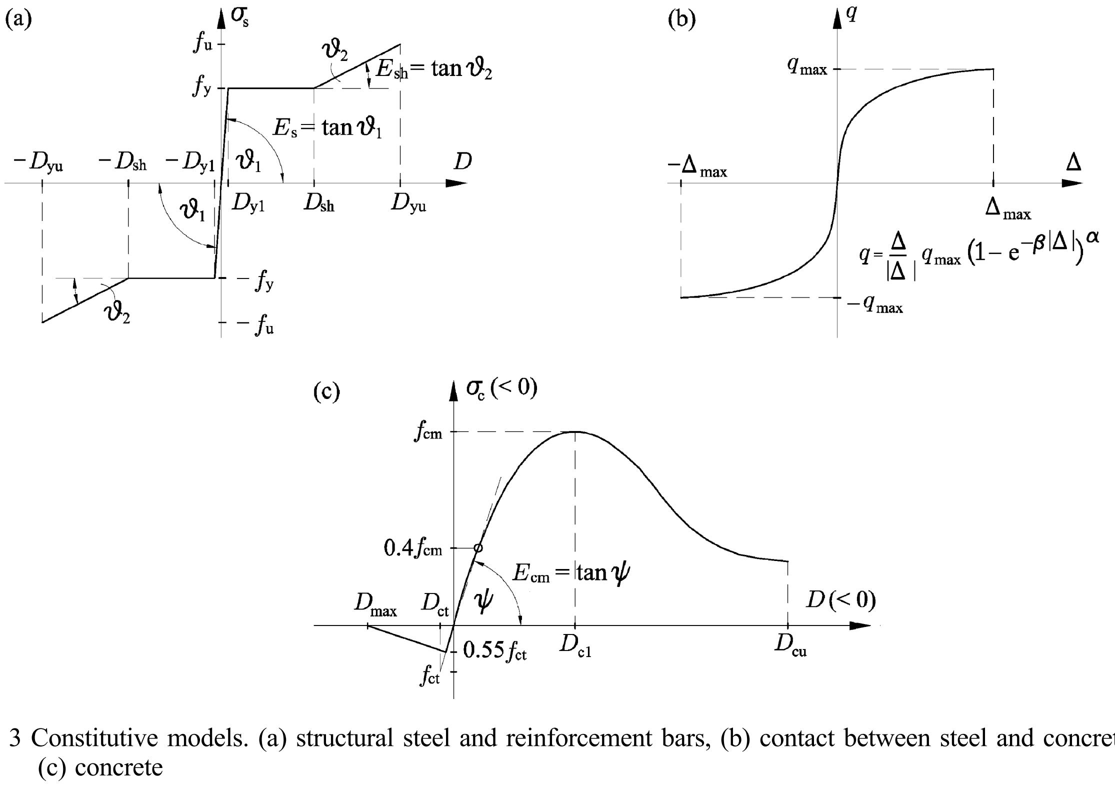

Fig. 3 Constitutive models. (a) structural steel and reinforcement bars, (b) contact between steel and concrete, (c) concrete

Table 1 Material parameters of concrete

Beam	f_{cm} [kN/cm^2]	D_{max}	D_{ct}	D_{c1}	D_{cu}
PI4	3:5	0	0	-0.00225	-0.021

Table 2 Material parameters of structural steel and reinforcement bars E_s=21 000 kN/cm^2, E_{sh}=0.008 E_s

Beam	f_y^{flange}	f_u^{flange}	f_y^{web}	f_u^{web}	f_y^{bars}	f_u^{bars}	D_{sh}
PI4	24.5*	36.1*	26.0*	37.2*	37.0*	37.5*	0.021

*kN/cm^2

Table 3 Material parameters of contact between reinforced concrete slab and steel girder

Beam	No. of Nelson's studs	α	β [cm^{-1}]	q_{max} [kN/cm]
PI4	18	0.800	7	4.68

The constitutive models for steel, concrete and the contact are presented in Fig. 3 in the form of graphs. All three models exibit a non-linear behaviour of materials and the connection. For structural steel and the reinforcing steel bars, a three-linear stress-strain diagram is used (Fig. 3a). The reinforced concrete slab and the steel girder are assumed to be connected with the standard Nelson studs having the diameter ϕ 19 mmand being welded in pairs to the upper flange of the steel girder. The studs are uniformly distributed along the contact. The generalized constitutive relation of the contact (in the literature it is called the 'shear flow-slip diagram') is such as suggested by Ollgaard *et al*. (1971) (Fig. 3b). The stress-strain diagram for concrete in compression of Desayi and Krishnan (1964) is used, and in tension as shown in Fig. 3(c). The extension of concrete stress-strain diagram into the tensile zone is taken from Bratina *et al*. (2004).

Abdel Aziz (1986) measured material parameters of structural steel, reinforcement bars and concrete and his findings are given in Tables 1, 2 and 3. The thickness of the concrete cover was, however, not given by Abdel Aziz (1986). We assumed that the distance between the centre of the reinforcement bars and the surface of concrete was 1.5 cm.

In our first analysis, we assume that the slip occurs over the actual contact surface of concrete and steel, in which case e=0. The concrete slab and the steel girder are connected with 9 pairs of the Nelson studs (see Fig. 6). The distance between the pairs of studs along the axis of the beam is thus 65 cm. The studs are modelled either as being continuously distributed along the axis (marked as 'continuous') or as being discrete ('discrete'). In the continuous case, the actual discrete placement of studs is replaced by the continuous tangent traction along the whole axis. In the discrete, discontinuous case, the effect of each stud is replaced by the constant tangent traction over the region occupied by the stud. This is achieved by the use of a specially designed finite element mesh, in which one very short, 20 mm long finite element is used to model the effect of each stud, and one or more long elements to model the region between the studs. The connection law in short elements representing the studs is assumed to follow the one by Ollgaard *et al*. (1971). No tangential connection between concrete and steel was assumed between the studs. We used the mesh with ten or more finite elements of type $E_{5\text{-}5}$ to model the whole beam for the continuous studs, and 22 elements $E_{5\text{-}5}$ for the discrete stud model ($E_{i\text{-}j}$ denotes the element type; i marks the number of interpolation points, and j the number of integration points in the element). The analyses employing more than ten or 22 elements exhibited no greater accuracy. Note

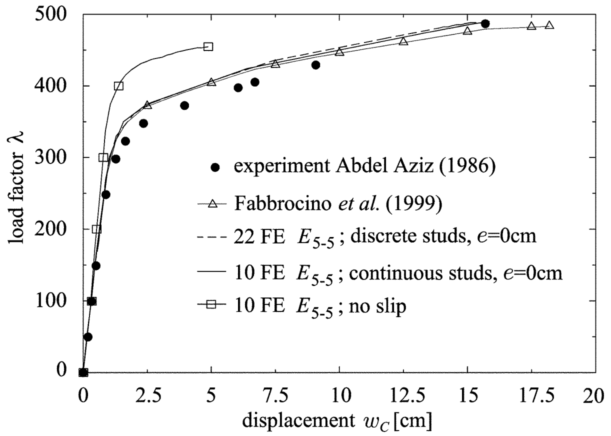

Fig. 4 Load-deflection curves of steel-concrete composite beam (e=0)

that 22 elements is the lowest possible number of elements to model the discrete placement of the studs. The load-displacement curves for the midspan deflection, w_C, are displayed in Fig. 4. A very good agreement between the calculated and experimentally found load-deflection curves for both the continuous and the discrete models can be observed. One can see that the results are also well in accord with the numerical results of Fabbrocino *et al.* (1999). The experimentally determined critical midspan deflection, $w_{C;cr}^{\exp}$, is 15.7 cm at the critical load $P_{cr}^{\exp}$ = 490 kN. The comparisons between the experimental and numerical values of the critical force P_{cr} and the critical midspan deflection are presented in Table 4. Fabbrocino *et al.* (1999) used the boundary element method and employed a very fine mesh to model the beam. Their calculated critical load is very close to the measured one, while their calculated midspan deflection $w_{C;cr}$ is overestimated for about 16% (Table 4). The error of our analysis is smaller: for the continuous studs, the error in the critical load P_{cr} is only 0.45%, and even a little smaller (0.40%) for the discrete studs. The midspan critical deflection error is null for the continuous model and 1.9% for the discrete model.

Figs. 5(a) and 5(b) show the slip distribution along the reference axis of the beam for the two load levels, λ=257 and λ=344. The slips, measured by Abdel Aziz (1986), those which were calculated by Fabbrocino *et al.* (1999), and the slips obtained by the present method for the continuous and discrete studs, are compared. Due to the symmetry of the geometry, supporting and the loading of the beam with respect to its centre, the slips are antisymmetric and are therefore presented in the figures only for the left half of the beam. The agreement between the results is good. Notice very small overall differences

Table 4 Comparisons between calculated and measured critical values of P_{cr} and $w_{C,cr}$ of steel-concrete composite beam (e=0)

	P_{cr} [kN]	$P_{cr} / P_{cr}^{\exp}$	$w_{C,cr}$ [cm]	$w_{C,cr} / w_{C,cr}^{\exp}$
Experiment Abdel Aziz (1986)	490	1.000	15.7	1.000
Fabbrocino *et al.* (1999)	486.3	0.993	18.20	1.159
10 FE $E_{5\text{-}5}$; continuous studs, e=0 cm	492.2	1.004	15.7	1.000
22 FE $E_{5\text{-}5}$; discrete studs, e=0 cm	488.0	0.996	15.4	0.981
10 FE $E_{5\text{-}5}$; no slip	452.8	0.924	4.6	0.293

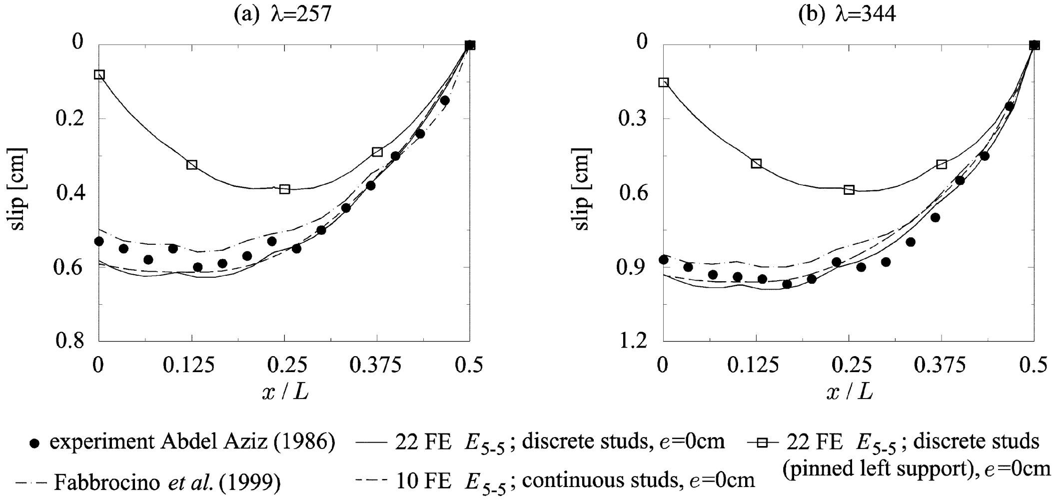

Fig. 5 Slip distribution along the composite beam axis for two load levels (e=0)

between the results of the continuous and discrete models, although in the discrete stud model, the curves are somewhat oscillating due to the assumed smoothness of the contact in regions between the studs.

The maximum vertical displacement was measured to be about 3% of the beam span. This indicates that the geometrically linear theory is sufficient for the analysis. The collapse of the beam, observed in the experiment, was triggered by large plastic deformations in the steel flange and consequent crushing of concrete at the point of application of the concentrated load. This indicates that the beam collapsed due to the failure of the cross-section. A similar collapse mechanism was predicted by our numerical analysis, in which highly localized plastic deformations in steel were followed by the softening of the concrete cross-section.

The forces in the studs at various loading stages are depicted in Fig. 6. The values of forces are given in relation to the ultimate bearing capacity of each stud. As you can see, the forces in studs at the moment of the global collapse of the beam are as high as 97% of their bearing capacity.

Next we analyse the effect of the generalized slip on the response of the beam. In Figs. 7 and 8 we show the variation of the generalized slip along the beam axis for e=0, 1, 2 and 3 cm for continuous (Fig. 7) and discrete (Fig. 8) studs. The results are shown for two loading stages, λ=257 and λ=344. It is apparent that parameter e somewhat effects the slip values. The comparison shows that e=2 cm offers the best fit to the experimental slip data.

The effect of the use of the generalized slip on the load-deflection diagram, the internal forces and the deformations in the beam is clearly very small. This is true for both continuous and discrete stud models. This fact is further illustrated in Figs. 9(b) and 9(c), showing the stress and strain distributions over the mid-point cross-section at P=452.8 kN.

It is instructive to show the results of analyses performed with the assumption that the righthand support is pinned, not free (see Fig. 2b). The analyses included the continuous and discrete studs and took e=0 cm. The results show that the pinning of the support has a negligible effect on the stiffness, bearing capacity and ductility of the beam. On the other hand, the pinning significantly effects the variation of the slip, see Fig. 5.

Finally, we show the results for the rigid connection between concrete and steel. The load-deflection curve is shown in Fig. 4 and in Table 4. We see that such a beam is considerably stiffer, and has a

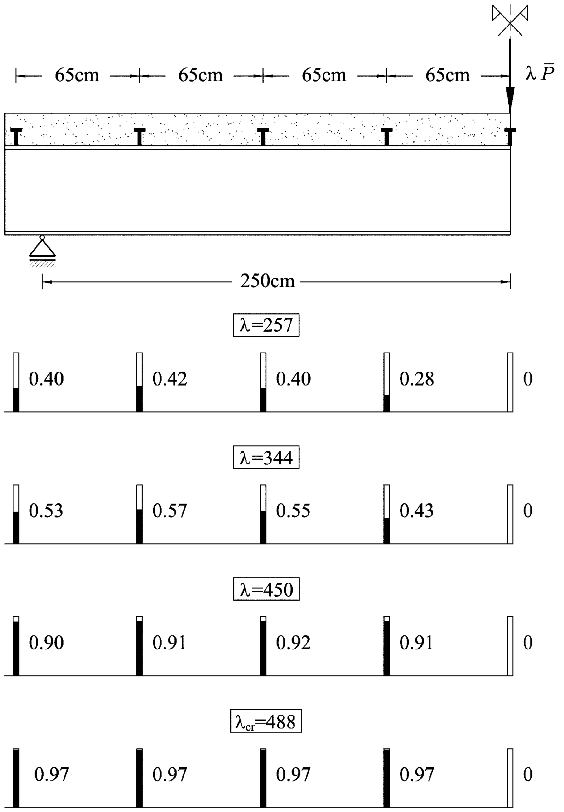

Fig. 6 Forces in studs at various loading stages (relative to their ultimate bearing capacity, $Q_{\max}$=130 kN)

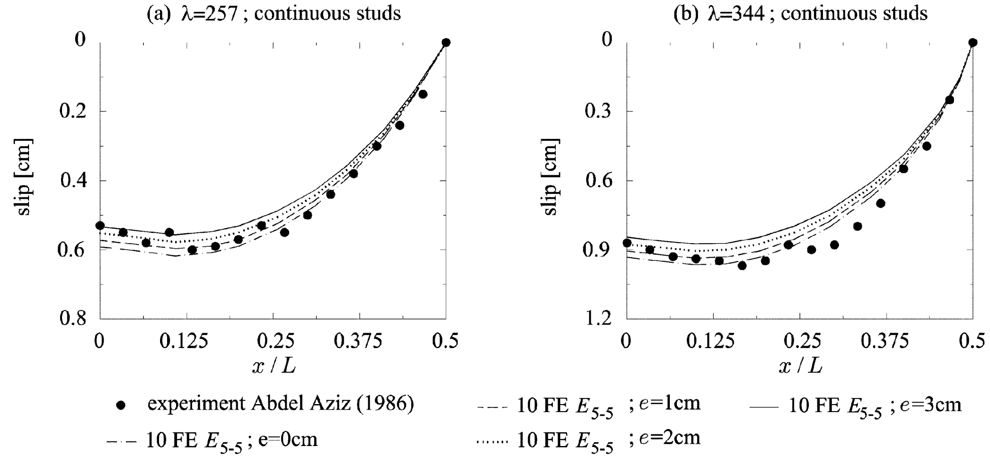

Fig. 7 Continuous studs. Slip distribution along the composite beam axis for e=0, 1, 2, 3 cm

smaller bearing capacity and a much smaller ductility than the beam with well designed shear studs. The stress and strain distributions over the mid-point cross-section are displayed in Fig. 9. The figure shows that a slightly bigger tension stresses develop in the lower steel flange and that a very large

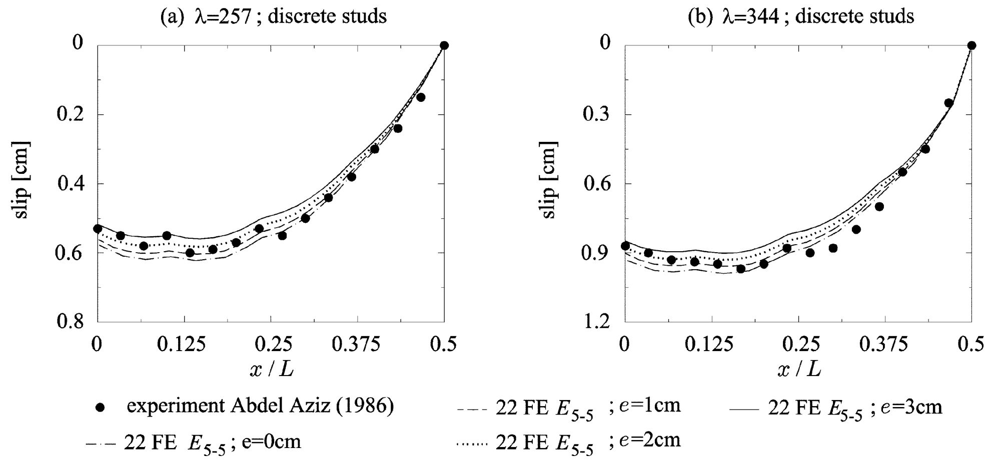

Fig. 8 Discrete studs. Slip distribution along the composite beam axis for *e*=0, 1, 2, 3 cm

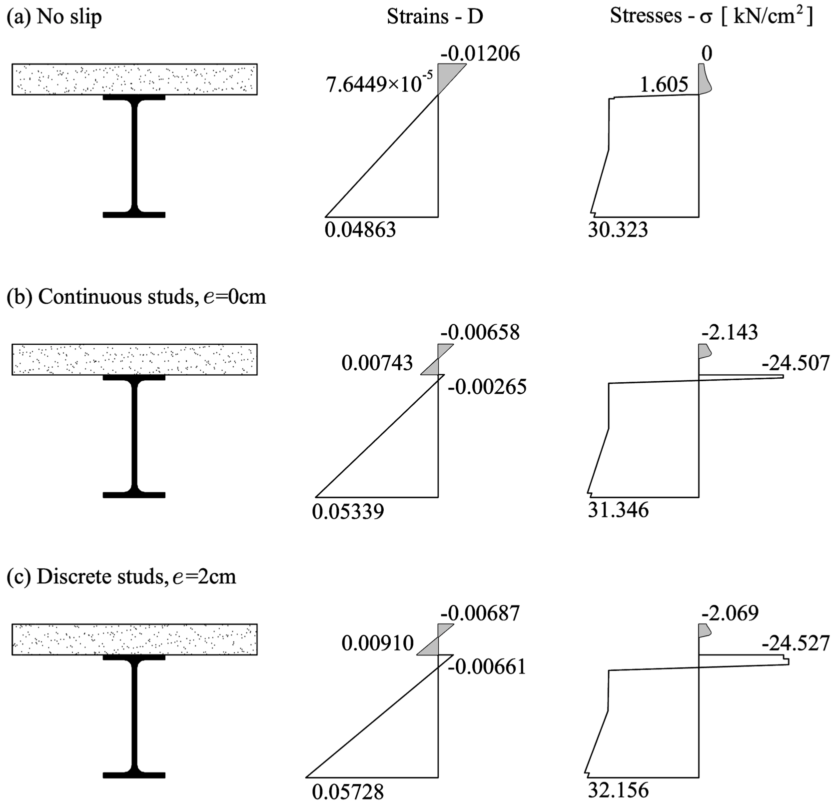

Fig. 9 Stress and strain distributions over the mid-point cross-section at *P*=452.8 kN

compression stresses (compared to the rigid connection case) appear in the upper steel flange in the case of the flexible connection.

5. Conclusions

We presented an effective, strain-based finite element method for the non-linear analysis of composite beams with flexible connections experiencing interlayer slips. The method is capable of modelling continuous or discrete connectors and makes it possible to account for the thickness of the sublayer, over which the slips occur. The formulation uses the geometrically linear planar beam theory, but its adaptation to the geometrically non-linear theory is also possible.

The accuracy and reliability of the method is demonstrated by the comparison of the results of our analysis of the steel-concrete composite beam with the experimental results of Abdel Aziz (1986) and the numerical results of Fabbrocino *et al*. (1999). The following conclusions can be drawn from these comparisons and results:

- The newly derived finite elements are accurate, robust and computationally efficient, and can be used to model both continuous and discrete studs.
- The numerical results show negligible differences between the results of continuous and discrete studs for the simply-supported composite beam subjected to a point load, as analysed here. This indicates that the model with continuously distributed studs probably suffices for the practical analysis of the steel-concrete composite beams. The continuous model is computationally more advantageous than the discrete one, because it needs much smaller number of finite elements to model the composite beam.
- The notion of the generalized slip introduced as an average slip over the connecting sublayer proved to be promising in determining the actual slip more accurately. Its effect on the stiffness, bearing capacity and ductility of the simply-supported composite beam subjected to a point force was found to be minor. Additional experimental and theoretical studies should be performed to exploit the idea further.

Acknowledgements

The work of B. Čas was financially supported by the Ministry of Education, Science and Sport of the Republic of Slovenia under contract S2-792-005/20157. The support is gratefully acknowledged.

References

Abdel Aziz, K. (1986), "Modèlisation et étude expérimentale de poutres mixtes acier-béton à connexion partielle ou espacé", PhD Thesis, Institut National des Sciences Appliquées des Rennes.

Adekola, A.O. (1968), "Partial interaction between elastically connected elements of a composite beam", *Int. J. Solids Struct*., **4**, 1125-1135.

Aribert, J.M. and Abdel Aziz, K. (1985), "Calcul des poutres mixtes jusqu'à l'état ultime avec un effet de soulèvement à l'interface acier-béton", *Constr. Métallique*, **4**, 3-41.

Ayoub, A. and Filippou, F.C. (2000), "Mixed formulation of nonlinear steel-concrete composite beam element", *J. Struct. Eng*., ASCE **126**(3), 371-381.

Ayoub, A. (2001), "A two-field mixed variational principle for partially connected composite beams", *Finite Element in Analysis and Design*, **37**, 929-959.

Bratina, S., Saje, M. and Planinc, I. (2003), "On materially and geometrically non-linear analysis of reinforced-concrete planar frames", *Int. J. Solids Struct*., **41**, 7181-7207.

Čas, B. (2004), "Non-linear analysis of composite beams with interlayer slip", PhD Thesis (in Slovene), University of Ljubljana, Faculty of Civil and Geodetic Engineering.

Čas, B., Saje, M. and Planinc, I. (2004), "Non-linear finite element analysis of composite planar frames with interlayer slip", *Comput. & Struct.*, accepted for publication.

Dall'Asta, A. and Zona, A. (2002), "Non-linear analysis of composite beams by displacement approach", *Comput. & Struct.*, **80**, 2217-2228.

Daniel, B.J. and Crisinel, M. (1993), "Composite slab behavior and strength analysis. Part I: Calculation procedure", *J. Struct. Eng.*, ASCE **119**(1), 16-35.

Desayi, P. and Krishnan, S. (1964), "Equation for the stress-strain curve of concrete", *J. Am. Concrete Institute*, **61**, 345-350.

Fabbrocino, G., Manfredi, G. and Cosenza, E. (1999), "Non-linear analysis of composite beams under positive bending", *Comput. & Struct.*, **70**, 77-89.

Fabbrocino, G., Manfredi, G. and Cosenza, E. (2000), "Analysis of continuous composite beams including partial interaction and bond", *J. Struct. Eng.*, ASCE **126**(11), 1288-1294.

Gattesco, N. (1999), "Analytical modeling of nonlinear behavior of composite beams with deformable connection", *J. Constr. Steel Research*, **52**, 195-218.

Gattesco, N. and Giuriani, E. (1996), "Experimental study on stud shear connectors subjected to cyclic loading", *J. Constr. Steel Research*, **38**(1), 1-21.

Girhammar, U.A., Gopu, V.K.A. (1993), "Composite beam-columns with interlayer slip-exact analysis", *J. Struct. Eng.*, ASCE, **119**(4), 1265-1282.

Newmark, N.M., Siess, C.P. and Viest, I.M. (1951), "Test and analysis of composite beams with incomplete interaction", *Proc. Soc. for Experimental Stress Analysis*, **9**, 75-92.

Ollgaard, J.G., Slutter, R.G. and Fisher, J.W. (1971), "Shear strength of stud connectors in lightweight and normal weight concrete", *AISC Eng. Journal*, **8**, 55-64.

Planinc, I. (1998), "A quadratically convergent methods of critical points determination of structures", PhD Thesis (in Slovene), University of Ljubljana, Faculty of Civil and Geodetic Engineering.

Ranzi, G., Bradford, M.A. and Uy, B. (2003), "A general method of analysis of composite beams with partial interaction", *Steel and Composite Structures*, **3**(3), 169-184.

Razaqpur, A.G. and Nofal, M. (1989), "A finite element for modeling the nonlinear behavior of shear connectors in composite structures", *Comput. & Struct.*, **32**(1), 169-174.

Robinson, H. and Naraine, K.S. (1988), "Slip and uplift effects in composite beams", *Proc. of ASCE Engineering Foundation Conference on Composite Construction*.

Salari, R., Spacone, E., Shing, P.B. and Frangopol, D.M. (1998), "Nonlinear analysis of composite beams with deformable shear connectors", *J. Struct. Eng.*, ASCE **124**(10), 1148-1158.

Vratanar, B. and Saje, M. (1998), "A consistent equilibrium in a cross-section of an elastic-plastic beam", *Int. J. Solids Struct.*, **36**, 311-337.

Wegmuller, A.W. and Amer, H.N. (1997), "Nonlinear response of composite steel-concrete bridges", *Comput. & Struct.*, **7**(2), 161-169.

DN